Science Advances

AAAS

advances.sciencemag.org/cgi/content/full/2/8/e1600157/DC1

# Supplementary Materials for

## Shock compression response of forsterite above 250 GPa

Toshimori Sekine, Norimasa Ozaki, Kohei Miyanishi, Yuto Asaumi, Tomoaki Kimura, Bruno Albertazzi, Yuya Sato, Youichi Sakawa, Takayoshi Sano, Seiji Sugita, Takafumi Matsui, Ryosuke Kodama

Published 3 August 2016, *Sci. Adv.* **2**, e1600157 (2016)
DOI: 10.1126/sciadv.1600157

**This PDF file includes:**

- fig. S1. Hugoniot and phase boundaries.
- fig. S2. The phase relations and Gibbs free energies as functions of pressure and temperature.
- fig. S3. A typical profile of decay for shot 37767.
- table S1. Measured quartz shock velocities and inferred Al states based on the impedance mismatching analysis.

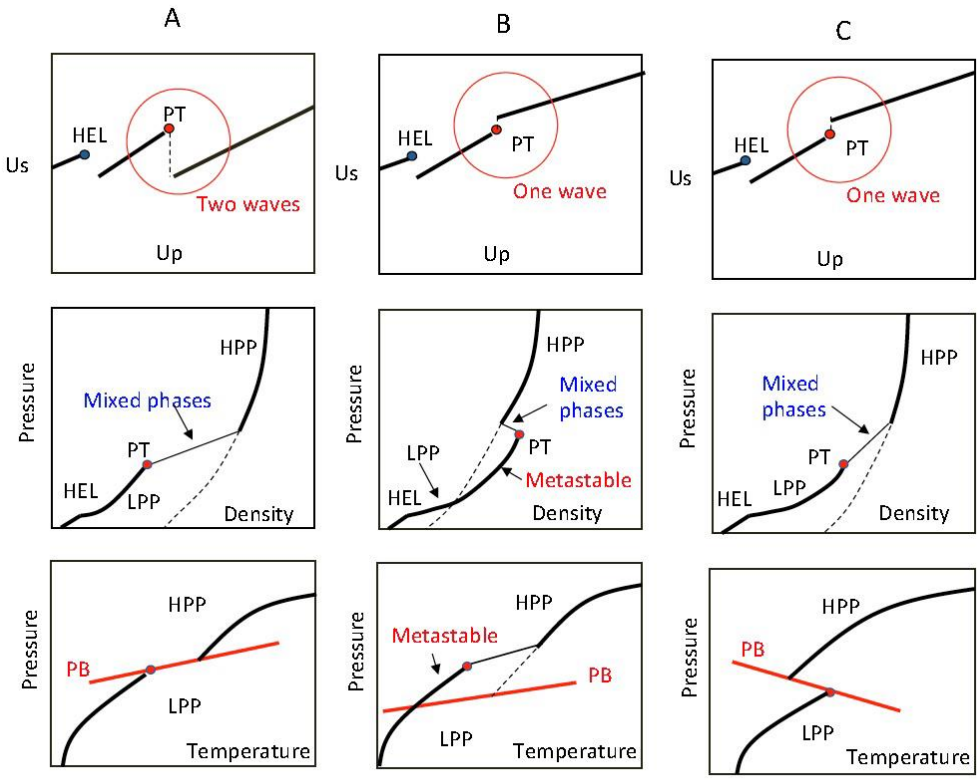


**fig. S1. Hugoniot and phase boundaries.** The relationships between shock velocity (Us) and particle velocity (Up), between pressure and density, and between pressure and temperature for three cases of phase transitions displaying (**A**) two-wave structure and positive phase boundary (PB), (**B**) one-wave structure and positive PB, and (**C**) one-wave structure and negative PB. HEL=Hugoniot elastic limit, PT=phase transition onset, LPP=low pressure phase, and HPP=high pressure phase.

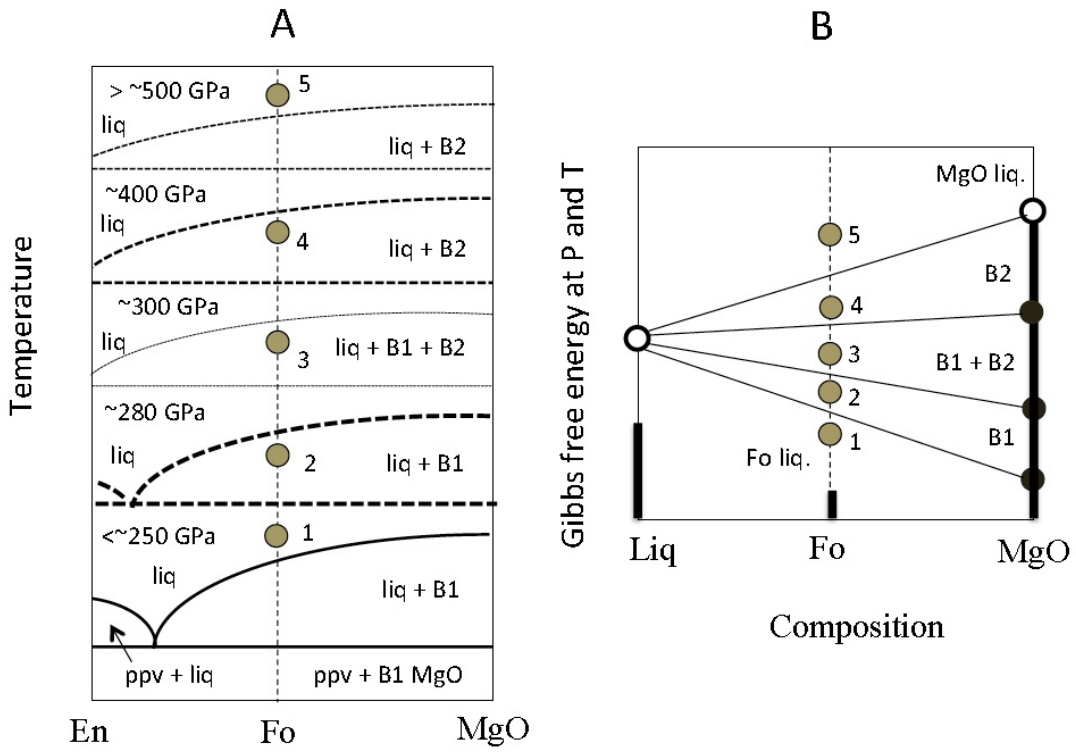


**fig. S2. The phase relations and Gibbs free energies as functions of pressure and temperature.** (**A**) Proposed eutectic phase relations in the system $MgSiO_3$ (En)-MgO at shock pressures of ~200 GPa to ~600 GPa, and (**B**) a comparison of the Gibbs free energy of Fo liquid relative to that for the Fo bulk composition mixture of a residual liquid (Liq) and MgO solid(s). Temperature at point 3 can be lower than that at point 2 due to the negative phase boundary between B1 and B2 MgO. Vertical heavy lines mean solids. The composition of Liq present is variable as illustrated in (A). For example, the compositions at points 1 and 5 are Fo, and those at points 2 - 4 are ~ 0.7 En. MgO is transformed from B1 to B2 structures as illustrated in Fig. 3. ppv=post-perovskite.

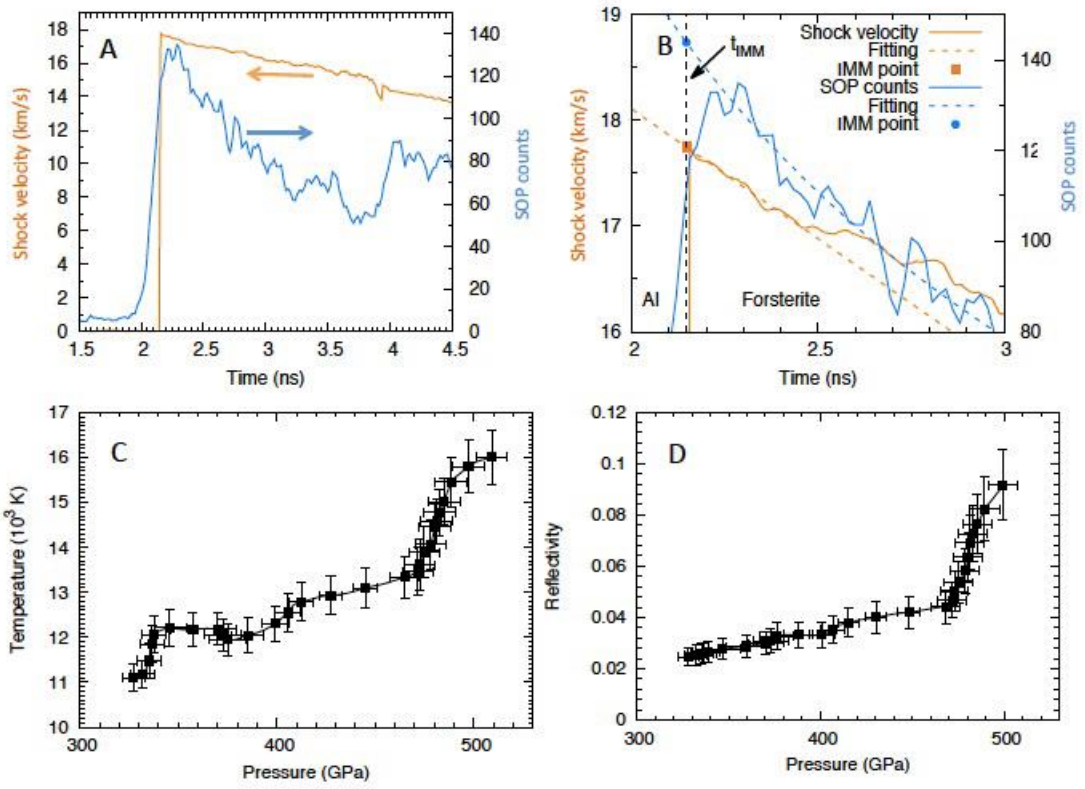


**fig. S3. A typical profile of decay for shot 37767.** (**A**) Shock velocity vs. time and thermal emission vs. time, (**B**) illustration of extrapolation to determine the shock velocity and emission count at Hugoniot point, (**C**) temperature-pressure relation, and (**D**) reflectivity-pressure relation. For Hugoniot measurement, shock velocity and emission count were read at the Fo-Al boundary, respectively, by a fitted curve for the measured profile in a limited time.

**table S1. Measured quartz shock velocities and inferred Al states based on the impedance mismatching analysis.**

| Shot number | Quartz shock velocity [km·s$^{-1}$] | Al pressure [GPa] | Al particle velocity [km·s$^{-1}$] |
|---|---|---|---|
| 33552 | 12.82±0.38 | 238.8 ± 19.5 | 6.36 ± 0.34 |
| 35283 | 13.14±0.21 | 251.9 ± 11.0 | 6.59 ± 0.19 |
| 33676 | 14.14±0.23 | 295.4 ± 12.9 | 7.29 ± 0.20 |
| 37817 | 15.57±0.15 | 364.4 ± 9.5 | 8.32 ± 0.14 |
| 37779 | 16.65±0.19 | 422.0 ± 12.8 | 9.11 ± 0.17 |
| 37767 | 17.43±0.21 | 466.7 ± 14.7 | 9.69 ± 0.19 |
| 36755 | 17.79±0.29 | 488.2 ± 20.5 | 9.96 ± 0.25 |
| 35314 | 19.59±0.35 | 604.6 ± 28.5 | 11.32 ± 0.31 |
| 35286 | 22.94±0.21 | 863.3 ± 20.7 | 13.96 ± 0.19 |

The one-sigma uncertainties are shown in the present experimental data. The uncertainties were directly calculated by accounting for the random measurement errors and systematic uncertainties of the quartz and aluminum references.